Université Paris-Saclay, LPTMS

Physics of Complex Systems

Une Application de la Théorie de Jeux en Champ Moyen à la Dynamique des Piétons

Matteo Butano

supervised by

Prof. Denis Ullmo

July 1, 2021

ABSTRACT

This thesis will focus on the topic of pedestrian dynamics. It will start presenting the experiment that inspired this research, performed in France and Argentina, that consisted in the analysis of the crowd's response to the passage of a cylindrical intruder in a controlled environment. The way this experiment contradicted expectations motivated the research of a theoretical explanation of what was observed. The research group I belong to tried to use Mean-Field Games (MFG) to explain the experiment. The second part of this thesis will therefore present the basis of MFG and its main features, with the description of the mathematical foundations and the physical interpretation of the results. Finally, the third part of this thesis reports the results we obtained in our attempt to model the experiment with Mean-Field Games. We will first explain the approach we chose to follow and then we will report the analytical solution and comment of the results. Given the simplicity of the model we used we are pretty happy with the results we obtained. There is still plenty to improve, but this is another story that will hopefully be told in the future.

Contents

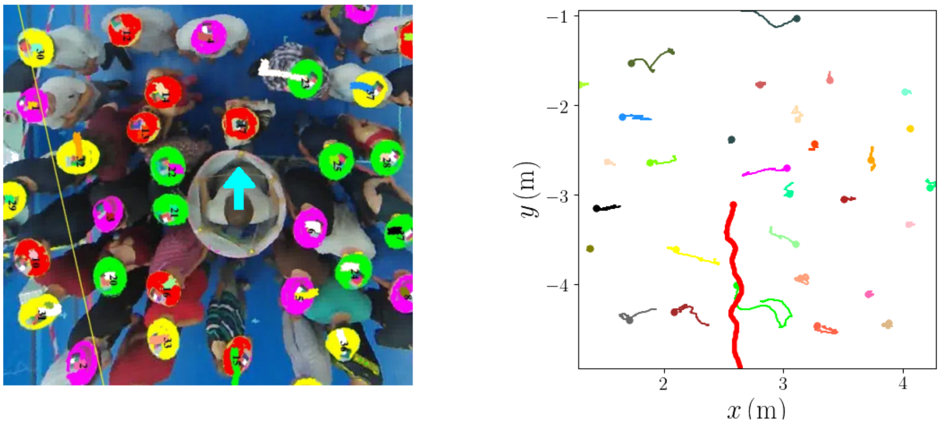

Figure 1: Snapshot of one of the performed experiments. The left figure shows the detection of participants using colored hats in Orsay, France. The right figure shows the numerical representation of the data. Images from [1]

1 The experiment

We all have experience with crowded environments. Although we did not always realize it, many of these spaces are designed on purpose to make us follow certain trajectories. Public spaces designers, in fact, have been using simulations to predict the flow of pedestrians for a long time. These predictions are then used to place wisely obstacles and doors, decide the length of corridors etc. in order to enhance safety. The underlying algorithms, however, are built to simulate human behavior using techniques of granular matter [17], [30], or fluid dynamics [28]. These approaches ultimately give reasonable results, but only for macroscopic quantities such as escape time, or to have a visual impression of the phenomenon. However, there are cases in which such models fail.

In 2019 the work of Nicolas et al. [1] reported a simple but very pedagogical example in which the usual pedestrian dynamics softwares would fail to predict the correct behavior of the crowd. Two experiments, performed in 2017 in Orsay (France) and Bariloche (Argentina) and involving between 35 and 40 participants of various ages, consisted in the analysis of the crowd's response to the presence of a single moving cylindrical obstacle. The crowd stood in a delimited square area and, with different pedestrian densities, the obstacle was made pass through. Figure 1 shows how the experiments were actually performed. One participant wore a cylinder, of diameter 74cm in France and 68 cm in Argentina, and walked his way through the crowd. Moreover, the people in the crowd were asked to

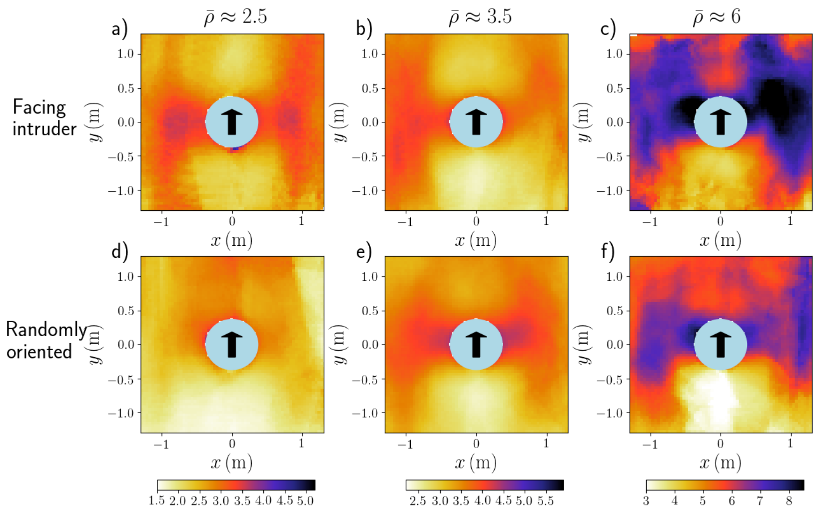

Figure 3: The density of pedestrians is displayed for three different average densities and in the two experimental set-ups: when people face the intruder they react more quickly than when they are oriented randomly, making space for the intruder and then closing behind him. Images from [1].

arrange in two configurations: in one case they were asked to face the intruder, in the other to stay in randomly oriented positions. If one attempts to simulate this situation considering pedestrians as granular matter, this would certainly fail. In fact, Seguin et al. showed in [2] what would happen if a cylinder was made pass through an area filled with granular particles. Figure 2 shows the main features of the simulation, that are the increase of the density in front of the cylinder and the appearance of an empty area behind it. These results are in clear disagreement with what was found by Nicolas and colleagues. In fact, as figure 3 shows, especially in the case in which pedestrians were asked to face the intruder, the experimental situation is quite different from what figure 2 might suggest. The density of pedestrians is indeed lower both in front and behind the cylinder, with a higher density at its sides, suggesting that people move laterally to

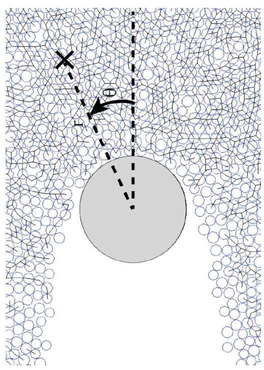

Figure 2: In [2], a cylinder passing through granular matter was simulated.

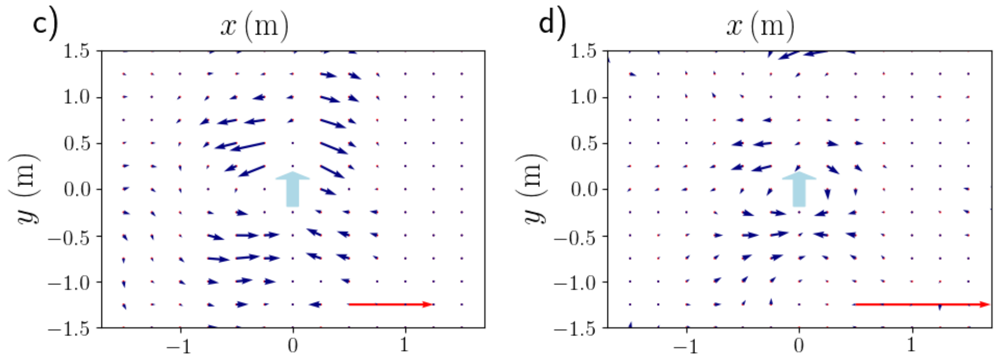

Figure 4: The figure shows the velocity field of pedestrians facing the intruder in case of sparse (left column, $\bar{\rho} \sim 1.5\,\mathrm{ped}/m^2$) and dense (right column, $\bar{\rho} \sim 6\,\mathrm{ped}/m^2$) environments. Images from [1].

avoid the incoming obstacle. This is confirmed when we observe in figure 4 the plots of the velocity field of the crowd. Right before the arrival of the intruder, people move laterally, giving up comfort by reaching a higher density area, but also avoiding impact. Then, after the obstacle has passed, the push of the crowd forces pedestrians to regain their position closing behind the cylinder. What is observed here is the ability of humans to *predict* the arrival of an obstacle. We do this because of individually acquired knowledge (we see the obstacle approaching) and also using environmental awareness (we feel others' motion and we are confirmed in our visual anticipation). The goal is then to find a theoretical description that can take into account both these aspects and translate them into simulations.

2 Mean-Field Games

Mean-Field Games (MFG) constitutes a relatively new field of research. Its foundations are in the works of J.-M. Lasry and P.-L. Lions [25], [26], [27] and of M. Huang, R. P. Malhamé and P. E. Caines [21]. During the years, many works have been focused on looking for existence and uniqueness of solutions [11], [19] and the comparison between discrete games in the limit of large number of players and their mean-field analogous [9], [14], [15]. At the same time, however, improvements were made towards the elaboration of numerical schemes [4], [7], [20], to solve MFG problems. Applications of MFG are found in various areas, such as finance [12], [16], economics [3], [5], social problems like pedestrian dynamics and segregation [6], [24], and also engineering [22], [23]. This list of results suggest how this topic has attracted the attention of many researches, as it did with mine when I chose what to focus my internship on. My work on the topic is based on the approach that D. Ullmo et al. explained clearly in [31] a couple of years ago. In this paper Ullmo and colleagues carefully explain how MFG can be linked to Quantum Mechanics (QM), in particular to the study of the Non-Linear Schrödinger Equation (NLSE), a very well established topic in Physics. The connection between the two fields, MFG and QM, is already quite interesting in itself, but what really struck me was that this approach does indeed work quite well, also considering that the nature of the phenomena explained is quite different!

2.1 The main equations

Mean-Field Games are optimally driven diffusive processes of a large number of agents. More explicitly, we consider a *differential game* that is played by a large number of *agents* N and that evolves in time. At each time t, we can associate to each agent its *state variable* $\vec{X}_i(t) \in \mathbb{R}^d$. Then, throughout the game, that starts at $t = 0$ and ends at $t = T$, every player has the possibility to change the *control parameter* $\vec{a}_i(t) \in \mathbb{R}^d$, that corresponds to the choice of a strategy. We then suppose that the evolution of a player's state variable is subjected to some noise and can therefore be described using using the *Langevin equation*

$$\dot{\vec{X}}_i = \vec{a}_i(t) + \sigma_i \vec{\xi}_i(t), \tag{1}$$

where $\vec{\xi}_i(t)$ is a d-dimensional vector of uncorrelated Gaussian white noises. In order to take the best decision about the strategy, agents select the drift term $\vec{a}_i$ by minimizing (maximizing) a certain cost (gain) functional, defined, for example in this case, as

$$c_i[\vec{a}](\vec{X}, t) = \mathbb{E}\left\{ \int_t^T \left[\frac{\mu}{2} (\vec{a}_i(\tau))^2 - V_i(\vec{X}(\tau), \tau) \right] d\tau + c_{Ti}(\vec{X}(T)) \right\}, \tag{2}$$

where $\vec{X}(t) = (\vec{X}_1(t), \ldots, \vec{X}_N(t))$ and $\vec{a} = (\vec{a}_1, \ldots, \vec{a}_N)$. There are various terms in equation (2) that need to be explained. First of all, c_T represents a *terminal cost* that each player knows from the beginning. Then, $V(\vec{X}, \tau)$ is a potential that acts on each player collectively and that describes how agents interact with each other and with the environment. Finally, the presence of the square of the control parameter $\vec{a}$ means that we are dealing with *quadratic games*, which have been widely described in [31]. This is not the only possible choice.

At this point some simplifications are in order. First of all, we assume that each player is identical, meaning that $\forall i$, $V_i = V$, $c_{Ti} = c_T$ and $\sigma_i = \sigma$.

Finally, the fundamental assumption that we make is that both the potential and the final cost depend on the players' positions only through the empirical density

$$\tilde{m}(\vec{x},t) = \frac{1}{N}\sum_{i=1}^{N}\delta(\vec{x}-\vec{X}_i(t)).$$

Then, we take the limit for a large number of players $N \to +\infty$. In this case, if we define $m(\vec{x},t) = \mathbb{E}[\tilde{m}(\vec{x},t)]$, we can then substitute $m(\vec{x},t)$ to $\tilde{m}(\vec{x},t)$. This means that we are not interested anymore in the description of every single trajectory, but in overall distribution of players in the space. The cost term can be now written as

$$c[\vec{a}](\vec{x},t) = \mathbb{E}\left\{\int_t^T \left[\frac{\mu}{2}(\vec{a}(\tau))^2 - V[m](\vec{x},\tau)\right] d\tau + c_T[m](\vec{x},T)\right\}. \quad (3)$$

Finally, the only type of potential we will consider is of the form

$$V[m](\vec{x},t) = gm(\vec{x},t) + U_0(\vec{x},t), \quad (4)$$

where g is a coupling term. A negative value of g makes the density term in the integral of equation (3) positive, and, if it must be minimized, this means that naturally the systems will adjust to a low density, resulting in *repulsive interactions*. Conversely, $g > 0$ means *attractive interactions*. Finally, we introduce the *value function*, obtained by minimizing the cost function

$$u(\vec{x},t) = \inf_{\vec{a}} c[\vec{a}](\vec{x},t). \quad (5)$$

At this point we are able to introduce the first of the two fundamental equations that describe the dynamics of a game. In order to do so however, we must think about the optimization of, for example, the path to reach point C from point A passing through point B. Because agents can optimize their strategy at any time, it is possible to show that optimizing the whole path gives the same result as joining together the paths obtained by optimizing separately the way from A to B and from B to C. This idea lies behind the *dynamic programming principle* [8], that allows us to write

$$u(\vec{x},t) = \inf_{\vec{a}} \mathbb{E}\left\{\int_t^{t+dt} \left[\frac{\mu}{2}(\vec{a}(\tau))^2 - V[m](\vec{x},\tau)\right] d\tau\right\} + u(\vec{x}+d\vec{x},t+dt), \quad (6)$$

that is called *Bellman equation*. Now we observe that

$$u(\vec{x}+d\vec{x},t+dt) \simeq u(\vec{x},t) + \frac{d}{dt}u(\vec{x},t)dt,$$

and the time derivative of the value function can be computed with *Ito chain rule* [18], obtaining

$$u(\vec{x}+d\vec{x},t+dt) \simeq u(\vec{x},t) + \left[\vec{\nabla}u \cdot \vec{a} + \partial_t u + \frac{\sigma^2}{2}\Delta u\right] dt. \tag{7}$$

Then, we can take the inf over $\vec{a}$ for both sides of the equation and obtain

$$u(\vec{x}+d\vec{x},t+dt) \simeq u(\vec{x},t) + \partial_t u dt + \frac{\sigma^2}{2}\Delta u dt + \left(\inf_{\vec{a}} \vec{\nabla}u \cdot \vec{a}\right) dt, \tag{8}$$

that we can substitute inside equation (6), giving

$$0 = \inf_{\vec{a}} \left[\frac{\mu}{2}(\vec{a}(t))^2 + \vec{\nabla}u \cdot \vec{a}(t)\right] + \partial_t u + \frac{\sigma^2}{2}\Delta u - V[m](\vec{x},t). \tag{9}$$

The optimal control can be easily evaluated by taking the d-dimensional derivative with respect to $\vec{a}$ of the expression in squared brackets and, putting it equal to zero, the solution is obtained and is equal to

$$\vec{a}^* = -\frac{\vec{\nabla}u}{\mu}, \tag{10}$$

which can be plugged back into equation (9) to obtain the *Hamilton-Jacobi-Bellman equation* (HJB).

$$\begin{cases} \partial_t u + \frac{\sigma^2}{2}\Delta u - \frac{(\vec{\nabla}u)^2}{2\mu} = V[m] \\ u(\vec{x},t=T) = c_T(\vec{x}) \end{cases} \tag{11}$$

This is a backward differential equation, that is built starting from its solution at time $t = T$

Now, given that each agent's position is supposed to evolve following a Langevin equation, the density of players satisfies

$$\partial_t m = \frac{\sigma^2}{2}\Delta m - \vec{\nabla} \cdot (m\vec{a}^*),$$

that is the *Fokker-Planck* equation. By substituting the value of the optimal control obtained in (10) we obtain

$$\begin{cases} \partial_t m - \frac{\sigma^2}{2}\Delta m + \frac{1}{\mu}\vec{\nabla} \cdot (m\vec{\nabla}u) = 0 \\ m(\vec{x},t=0) = m_0(\vec{x}) \end{cases} \tag{12}$$

Equations (11) and (12) constitute a backward-forward system. Starting from an initial density value, HJB equation informs FPE on incoming events. In fact, after HJB chooses the best possible value function, the FPE finds the next best density. It is in this process of interaction between the two equation that lies the predictive ability of MFG. We will see this in more details in the following.

2.2 Changes of variables

Now that we have built all the tools of MFG, we are left with a set of coupled equations which is not trivial to solve. A very wise approach has been devised in [31], where a *Cole-Hopf transformation* is performed and the problem is cast in a more familiar setting for many physicists. In fact, let us considers the transformation

$$u(\vec{x},t) = -\mu\sigma^2 \log \Phi(\vec{x},t), \tag{13}$$

and substitute into equation (11). We then get to the equation

$$\mu\sigma^2 \partial_t \Phi = -\frac{\mu\sigma^4}{2}\Delta\Phi - V[m]\Phi, \tag{14}$$

a standard heat equation, with terminal condition

$$\Phi(\vec{x}, t = T) = e^{-\frac{c_T(\vec{x})}{\mu\sigma^2}}. \tag{15}$$

Now we can also define

$$\Gamma(\vec{x},t) = \frac{m(\vec{x},t)}{\Phi(\vec{x},t)}, \tag{16}$$

that, when substituting into equation (12), gives

$$\mu\sigma^2 \partial_t \Gamma = \frac{\mu\sigma^4}{2}\Delta\Gamma + V[m]\Gamma. \tag{17}$$

Equations (14) and (17) only differ by a change in sign while containing all the information of the original MFG equations. The one we just performed is not the only change of variable that can be done to transform mean-field game equations into something already seen in other fields of Physics. As explained in [29], we can also perform a Madelung like change of variables defining $K(\vec{x},t)$ such that $\Phi(\vec{x},t) = \sqrt{m(\vec{x},t)}e^{K(\vec{x},t)}$ and $\Gamma(\vec{x},t) = \sqrt{m(\vec{x},t)}e^{-K(\vec{x},t)}$, that substituting in equations (14) and (17) gives

$$\begin{cases} \partial_t m + \vec{\nabla}\cdot(m\vec{v}) = 0, \\ \partial_t \vec{v} + \vec{\nabla}\left[\frac{\sigma^4}{2\sqrt{m}}\Delta\sqrt{m} + \frac{v^2}{2} + \frac{V[m]}{\mu}\right] = 0, \end{cases} \tag{18}$$

where $\vec{v}$ is the velocity of agents and is defined as

$$\vec{v} = \frac{\sigma^2}{2m}\left(\Gamma\vec{\nabla}\Phi - \Phi\vec{\nabla}\Gamma\right) = -\frac{\vec{\nabla}u}{\mu} - \sigma^2\frac{\vec{\nabla}m}{2m}. \tag{19}$$

This is called *hydrodynamic representation*. In particular, the first equation of system (18) is a continuity equation. We conclude this general introduction about MFG by mentioning the important results reported by P. Cardialaguet et al. in [13]. In this work, in fact, the limit of large ending time $T \to +\infty$ is considered. Under the hypothesis that there is no explicit time dependence in the cost function (2), it was proved that an *ergodic solution* exists and it is valid for $0 << t << T$. This solution is of the form $(m^e(\vec{x}), u^e(\vec{x}) + \lambda_e t)$ where $m^e(\vec{x})$ and $u^e(\vec{x})$ satisfy the equations

$$\begin{cases} -\lambda_e + \frac{\sigma^2}{2}\Delta u^e - \frac{(\vec{\nabla} u^e)^2}{2\mu} = V[m^e] \\ \frac{\sigma^2}{2}\Delta m^e + \frac{1}{\mu}\vec{\nabla}\cdot(m^e\vec{\nabla}u^e) = 0 \end{cases} \tag{20}$$

In the Schrödinger representation the ergodic solutions are

$$\Phi^e = e^{-\frac{u^e}{\mu\sigma^4}}, \quad \Gamma^e = \frac{m^e}{\Phi^e}, \tag{21}$$

and it easy to prove that they both follow the equation

$$\lambda_e \psi^e = -\frac{\mu\sigma^4}{2}\Delta\psi^e - V[m]\psi^e. \tag{22}$$

Most importantly, the knowledge of the ergodic solution gives access to the solution also of the time dependent problem, because it is possible to show that

$$\Phi(\vec{x}, t) = \exp\left\{\frac{\lambda_e}{\mu\sigma^2}t\right\}\psi^e(\vec{x}), \quad \Gamma(\vec{x}, t) = \exp\left\{-\frac{\lambda_e}{\mu\sigma^2}t\right\}\psi^e(\vec{x}) \tag{23}$$

solve equations (14) and (17) respectively.

3 MFG model of the experiment

So far we have described in details the foundation of MFG and their mathematical structure. The way we want to apply them to the experiment of Nicolas et colleagues is by considering the parameter $\vec{a}(t)$ as the velocity of pedestrians. We think this approach is reasonable because the only thing a person has to decide at each instant when walking through a crowd is their velocity. Module and direction of the velocity will indeed determine the motion. Pedestrians optimize their velocity according to the density around them and the obstacles they encounter. Moreover, since crowded environments change quickly and a pedestrian has to adapt to many small perturbation, it also seems appropriate to describe the motion of a single person in the crowd with the Langevin equation (1). This is why we thought MFG could apply well to this situation.

3.1 Passing to the moving frame

The problem we are trying to model is the evolution of the density of pedestrians in a confined environment, namely a square of side L, through which a cylinder is made pass from bottom to top with constant velocity $\vec{s} = (0, s)$. We argue then that the right set of equations to describe this problem is given by MFG equations in the NLS representation that we recall

$$\mu\sigma^2\partial_t\Phi = -\frac{\mu\sigma^4}{2}\Delta\Phi - V[m]\Phi,$$
$$\mu\sigma^2\partial_t\Gamma = \frac{\mu\sigma^4}{2}\Delta\Gamma + V[m]\Gamma,$$

where in this case $V[m] = gm(\vec{x}, t) + U(\vec{x}, t)$ with $U(\vec{x}, t)$ representing the moving cylinder as an external potential equal to $+\infty$ inside a 2 dimensional disk of radius R and equal to 0 outside. This external potential introduces an explicit time dependence in the cost function (2), preventing the existence of an ergodic state. To correct this problem we pass from the point of view of the laboratory to the point of view of the cylinder. In order to do so we define of the following quantities

$$\tilde{u}(\vec{x} - \vec{s}t, t) = u(\vec{x}, t), \quad \tilde{m}(\vec{x} - \vec{s}t, t) = m(\vec{x}, t),$$
$$\tilde{\Phi}(\vec{x} - \vec{s}t, t) = \Phi(\vec{x}, t), \quad \tilde{\Gamma}(\vec{x} - \vec{s}t, t) = \Gamma(\vec{x}, t).$$

In this framework the potential does not depend on time anymore and it becomes $\tilde{V}[\tilde{m}] = g\tilde{m} + \tilde{U}(\vec{x})$, with

$$\tilde{U}(\vec{x}) = \begin{cases} +\infty & x < R \\ 0 & \text{otherwise} \end{cases}. \tag{24}$$

For all other quantities the time dependence now appears also in the position variable. In this case we observe that

$$\partial_t f(\vec{x}, t) = \frac{\mathrm{d}}{\mathrm{d}t} f(\vec{x}, t) = \frac{\mathrm{d}}{\mathrm{d}t}\tilde{f}(\vec{x} - \vec{s}t, t) = \partial_t\tilde{f} - \vec{s}\cdot\vec{\nabla}\tilde{f}. \tag{25}$$

We can then substitute expression (25) into equations (14) and (17) and obtain the moving frame equations

$$\mu\sigma^2\partial_t\tilde{\Phi} - \mu\sigma^2\vec{s}\cdot\vec{\nabla}\tilde{\Phi} = -\frac{\mu\sigma^4}{2}\Delta\tilde{\Phi} - V[m]\tilde{\Phi}, \tag{26}$$

$$\mu\sigma^2\partial_t\tilde{\Gamma} - \mu\sigma^2\vec{s}\cdot\vec{\nabla}\tilde{\Gamma} = \frac{\mu\sigma^4}{2}\Delta\tilde{\Gamma} + V[m]\tilde{\Gamma}. \tag{27}$$

We want to find the ergodic state of the moving frame equations. Recalling now the relationship between the ergodic state solution and the time dependent one expressed in (23), we observe that

$$\partial_t \tilde{\Phi} = \frac{\lambda_e}{\mu\sigma^2}\tilde{\Phi} = \frac{\lambda_e}{\mu\sigma^2} e^{\frac{\lambda_e}{\mu\sigma^2}t}\tilde{\Phi}^e, \quad \partial_t \tilde{\Gamma} = -\frac{\lambda_e}{\mu\sigma^2}\tilde{\Gamma} = -\frac{\lambda_e}{\mu\sigma^2} e^{-\frac{\lambda_e}{\mu\sigma^2}t}\tilde{\Gamma}^e.$$

These expressions can finally be substituted inside equations (26) and (27) to get rid of any explicit time dependence. Simplifying all the exponentials we finally obtain

$$\frac{\mu\sigma^4}{2}\Delta\tilde{\Phi}^e - \mu\sigma^2\vec{s}\cdot\vec{\nabla}\tilde{\Phi}^e + \tilde{V}[\tilde{m}^e]\tilde{\Phi}^e = -\lambda_e\tilde{\Phi}^e, \tag{28}$$

$$\frac{\mu\sigma^4}{2}\Delta\tilde{\Gamma}^e + \mu\sigma^2\vec{s}\cdot\vec{\nabla}\tilde{\Gamma}^e + \tilde{V}[\tilde{m}^e]\tilde{\Gamma}^e = -\lambda_e\tilde{\Gamma}^e. \tag{29}$$

These equations contain no time dependent quantities anymore. The last problem to solve before starting devising a numerical scheme to solve the equations is to find the right boundary conditions in order to fix the solutions.

3.2 Choosing boundary condition

In order to solve equations (28) and (29), it is important to understand what boundary conditions to impose in order to fix a solution. In the experiment of the moving cylinder, far from it people were not moving, meaning that, far from the obstacle, the velocity of the pedestrians was null in the laboratory frame. This means that, when passing to the moving frame, agents at the boundary should move with velocity $-\vec{s}$. From the hydrodynamic representation (18) of MFG, one knows that the definition of velocity in terms of Φ and Γ is

$$\vec{v} = \frac{\sigma^2}{2m}\left(\Gamma\vec{\nabla}\Phi - \Phi\vec{\nabla}\Gamma\right) = -\frac{\vec{\nabla}u}{\mu} - \sigma^2\frac{\vec{\nabla}m}{2m}. \tag{30}$$

This definition is valid also if we consider the ergodic state of the moving frame

$$\vec{v} = \frac{\sigma^2}{2\tilde{m}^e}\left(\tilde{\Gamma}^e\vec{\nabla}\tilde{\Phi}^e - \tilde{\Phi}^e\vec{\nabla}\tilde{\Gamma}^e\right) = -\frac{\vec{\nabla}\tilde{u}^e}{\mu} - \sigma^2\frac{\vec{\nabla}\tilde{m}^e}{2\tilde{m}^e}. \tag{31}$$

Now, we know that at the boundary the density should be constant therefore we can drop the gradient of $\tilde{m}^e$ in the last expression; this means that we can just force the equality

$$\frac{\vec{\nabla}\tilde{u}^e}{\mu} = \vec{s}, \tag{32}$$

in order to have the right velocity far from the obstacle. Now, recalling that $\tilde{u}^e = -\mu\sigma^2 \log \tilde{\Phi}^e$, we can substitute in equation (32) and obtain

$$\sigma^2 \frac{\vec{\nabla}\tilde{\Phi}^e}{\tilde{\Phi}^e} = -\vec{s},$$

from which we obtain the equations

$$\frac{\partial \tilde{\Phi}^e}{\partial x} = 0, \quad \frac{\partial \tilde{\Phi}^e}{\partial y} = -\frac{s}{\sigma^2}\tilde{\Phi}^e,$$

that can be solved yielding the ergodic asymptotic solution

$$\tilde{\Phi}^e(x, y) = Ce^{-\frac{s}{\sigma^2}y}. \tag{33}$$

In order to fix C, we observe that far from the cylinder the density should be the average one, that we call m_0. Therefore, recalling that $\tilde{\Phi}^e\tilde{\Gamma}^e = \tilde{m}^e$, we can take $C = \sqrt{m_0}$ and thus have that $\tilde{\Gamma}^e(x, y) = \sqrt{m_0}e^{\frac{s}{\sigma^2}y}$. An interesting thing we notice is that a new parameter has emerged, one that relates the diffusion coefficient and the velocity of the cylinder. We will call this parameter $f = \frac{s}{\sigma^2}$. This boundary solutions contain all the information necessary to find the solution to the entire equations, since the only conditions Φ and Γ have to satisfy at the boundary are those related to the velocity and the value of the average density.

Having found the expression of the asymptotic solution not only gives us the boundary conditions to solve the equations; in fact, it also allows us to fix λ_e, giving us the correct ergodic state. Since λ_e is a constant quantity it can be computed using the asymptotic solution and we are sure it will also be valid for the general solution. To fix the parameter λ_e, we can indeed substitute the asymptotic form (33) into (28), which has to be valid far from the cylinder. This leads to

$$\frac{\mu\sigma^4}{2}\frac{s^2}{\sigma^4}\tilde{\Phi}^e + \mu\sigma^2\frac{s^2}{\sigma^2}\tilde{\Phi}^e + gm_0\tilde{\Phi}^e = -\lambda_e\tilde{\Phi}^e, \tag{34}$$

giving

$$\lambda_e = -gm_0 - \frac{3}{2}\mu s^2 . \tag{35}$$

3.3 Numerical solution

Now that we have solved the problem of boundary conditions, our goal is to find a numerical scheme to solve the equations. Let us consider equation (28).

$$\frac{\mu\sigma^4}{2}\Delta\tilde{\Phi}^e - \mu\sigma^2\vec{s}\cdot\vec{\nabla}\tilde{\Phi}^e + \tilde{V}[\tilde{m}]\tilde{\Phi}^e = -\lambda_e\tilde{\Phi}^e.$$

We will use the cylindrical potential (24), implemented numerically as $\tilde{V}_0 V(\vec{x})$

$$V(\vec{x}) = \begin{cases} 1 & x < R \\ 0 & \text{otherwise} \end{cases} . \tag{36}$$

Then, we first consider $g = 0$, therefore the equation we have to solve numerically are

$$\frac{\mu\sigma^4}{2}\Delta\Phi - \mu\sigma^2 s\partial_y\Phi + V_0V(\vec{x})\Phi = -\lambda\Phi, \tag{37}$$

where we dropped the tilde and the denotation of ergodic state, and already used the fact that the velocity of the cylinder is vertical. Now we are ready to implement the numerical scheme. We want to solve the equation on a box of side L, therefore, first of all, we define a meshgrid in Python of $N\times N$ points corresponding to the (x, y) coordinates in Euclidean space. Then we define the matrixces $\Phi\in\mathbb{R}^{N,N}$ and $\Gamma\in\mathbb{R}^{N,N}$ that we have to evaluate. We will then use the meshgrid matrix of coordinates to plot the values of the two matrices Φ and Γ. In order to do this, we first write the discrete form of equation (37)

$$\frac{\mu\sigma^4}{2dx^2}(\Phi_{i-1,j}+\Phi_{i+1,j}+\Phi_{i,j-1}+\Phi_{i,j+1}-4\Phi_{i,j})-\mu\sigma^2 s\frac{\Phi_{i,j+1}-\Phi_{i,j-1}}{2dy}+V_0V_{i,j}\Phi_{i,j} = -\lambda\Phi_{i,j},$$

where we choose $dx = dy$. Then make the term $\Phi_{i,j}$ explicit and obtain

$$\Phi^{k+1}_{i,j} = \frac{\frac{\mu\sigma^4}{2}(\Phi^k_{i-1,j}+\Phi^k_{i+1,j}+\Phi^k_{i,j-1}+\Phi^k_{i,j+1}) - \frac{\mu\sigma^2}{2}sdx(\Phi^k_{i,j+1}-\Phi^k_{i,j-1})}{2\mu\sigma^4-\lambda dx^2 - V_0V_{i,j}dx^2}.$$

This is the recursive rule that updates $\Phi_{i,j}$ until convergence. Starting from an initial guess of the solution, but with boundary conditions given by solution (33), the algorithm updates all the points of the Φ matrix simultaneously, just shifting rows or columns to sum neighboring points. At each step, the relative distance with the matrix at the previous iteration is computed and the algorithm halts as soon as a threshold is reached. This method is called Jacobi method and in practice it takes the initial guess for the solution and it connects it smoothly to the boundary conditions while solving the equation. The same can be done for Γ, just changing sign of s. Now that we have found both Φ and Γ, we can also solve the case for $g \neq 0$. We do this by starting with an initial density matrix with all entries equal to m_0. Then, we use the Jacobi method to compute Φ and Γ but this time also including the density term. Finally, we just use that $m = \Phi\Gamma$, update the density and compute again Φ and Γ. We repeat this operation until convergence of m.

3.4 Results

Let us start by defining some key quantities. First of all, in the two dimensional setting we framed our problem in, it is possible to define the *kinetic energy* and the *interaction energy* as, respectively,

$$E_{kin} = \frac{\mu\sigma^4}{2\nu^2}, \quad E_{int} = g\bar{\rho}.$$

In the definition of the kinetic energy we introduced ν, that is the *healing length*. This, as explained in [10], corresponds to the distance after which a perturbed density of pedestrian recovers its bulk value. This emerges from the balance between interaction and diffusion. Therefore, equating the two energies just defined we obtain

$$\nu = \sqrt{\frac{\mu\sigma^4}{2|g|m_0}}. \tag{38}$$

Then, it is also possible to define the *healing time* $\tau = |\mu\sigma^2/g\bar{\rho}|$, which is the time required for the solution to recover from a perturbation. These two quantities can then be used to obtain another important length of the problem: the *healing speed*, defined as

$$\xi = \frac{\nu}{\tau} = \sqrt{\frac{|g|m_0}{2\mu}}, \tag{39}$$

that quantify the speed of recovery of the density of pedestrians to its bulk value. We can use the healing speed and the healing length to describe all possible scenarios we can deal with in this setting, given that ξ and ν are both defined in terms of g and that once we fix both the size of the room and the size of the obstacle we can tune the other parameters μ and σ independently. Figure 5 shows the 4 main regimes we can find our solution in. Figure 5a shows the case $\xi > s, \nu > R$, in which the crowd adjusts easily to the passage of the obstacle, thanks to a healing speed larger than

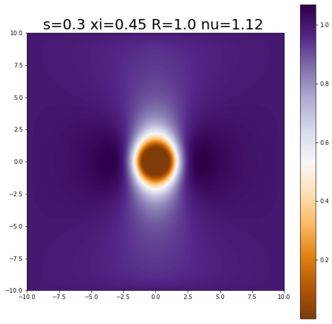

(a) $\xi > s, \nu > R$

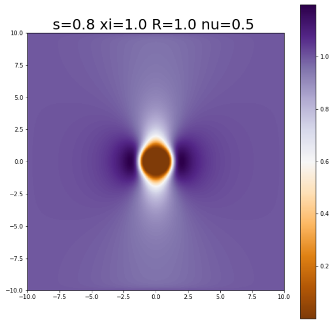

(b) $\xi > s, \nu < R$

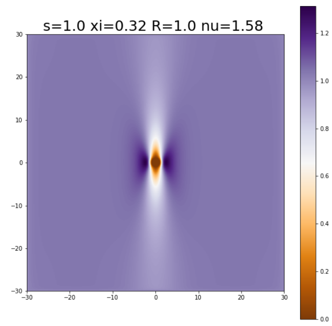

(c) $\xi < s, \nu > R$

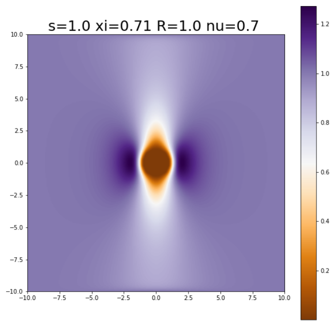

(d) $\xi < s, \nu < R$

Figure 5: The relations between healing length, healing speed and the velocity and size of the obstacle identify four different regimes.

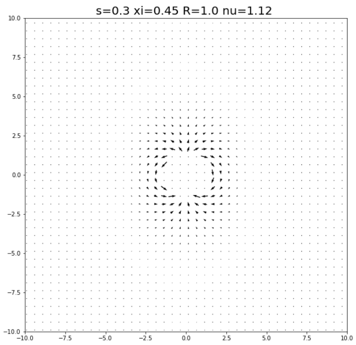

(a) $\xi > s, \nu > R$

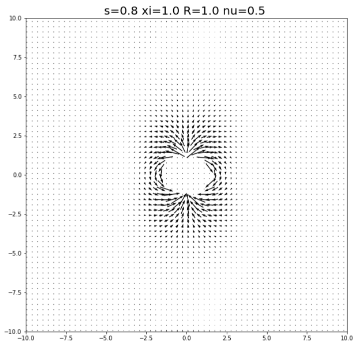

(b) $\xi > s, \nu < R$

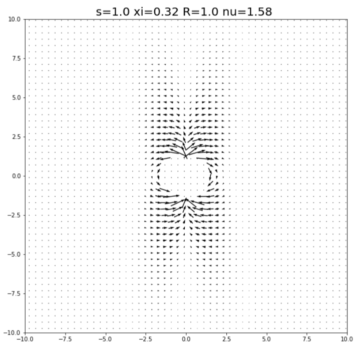

(c) $\xi < s, \nu > R$

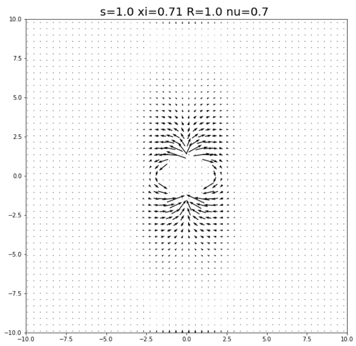

(d) $\xi < s, \nu < R$

Figure 6: The relations between healing length, healing speed and the velocity and size of the obstacle identify four different regimes, velocity plots.

the speed of the intruder. In figure 5b, on the other hand, a healing length smaller than the size of the cylinder means that only those in its proximity are impacted. In this case we can see the darker shadows at the sides of the obstacle, corresponding to an increase in density: pedestrians make space for the intruder as soon as they encounter it, with little anticipation. Figures 5c and 5d show the case in which the $\xi < s$. We see in this case that people make space for the incoming intruder much earlier than in the $\xi > s$ case, effectively showing some degree of anticipation. How far in space the perceived presence of the obstacle causes the crowd to start moving is determined by the value of the healing length. These observations are confirmed and amplified when the velocity field of pedestrian is analyzed as figure 6 shows. In figure 6a we see how only people in the vicinity of the obstacle are affected by it, and they move relatively slowly to adjust to its presence. Moreover, we see people moving in an almost circular region around the cylinder. This feature is displayed even better in figure 6b, where the pattern of motion is again of a radial displacement, but the concerned area is clearly larger. We link this behavior to the fact hat in both cases $\xi > s$, giving pedestrians the possibility to start reacting just when they start feeling the pressure from the incoming cylinder, without hurrying much. In fact, in figures 6c and 6d we see how $\xi < s$ implies the emergence of anticipation patterns. The two pictures show that people start reacting already far away from the obstacle, moving laterally to make room for its passage. Then, they escape the crowd's pressure filling the empty space behind the cylinder. Moving laterally then seems to be the least expensive move to perform in this context, and intuitively this makes sense, because, while being the shortest possible displacement to avoid the cylinder, it also puts the agent under the smallest possible pressure from surrounding people.

4 Conclusions

From what we have seen so far, we are pretty happy with our results. In fact, the passage to the moving frame not only allowed us to obtain equations easier to solve, namely equations (28) and (29), but the results it produced are qualitatively very promising. Despite the simplicity of the model, the overall behavior represented by our solution shows both of the experiment's main features, namely the ability of pedestrians to anticipate the obstacle and their reaction to the pressure from others. Since we believed that our approach could be pushed even further, we also tried to get as close as possible to the quantitative behavior. We tuned the parameter σ, μ and g in order to obtain something similar to what was obtained in the experiment. In particular, we tried to match the density shown in figure 7a and the corresponding velocity displayed in 7c. We assumed that the cylinder moved at $0.75 m/s$, half the average human walking speed. The result is quite good. As we can see in figure 7b, additionally to the already commented qualitative agreement, we recover a value of the density of $\sim 4,6\,\text{ped}/m^2$ at the sides of the obstacle, not exactly the same but close to what is found in the experiment. Then, figure 7d shows the velocity field we obtained using our simulation. Plotting the velocity was not an easy task. In fact, due to the finite nature of the algorithm, some agents are considered as almost *under* the cylinder. Since these points will try to escape from it at very high velocity, plotting the simulated velocity of pedestrian in the vicinity of the intruder would result in a bunch of long arrows without any physical meaning. In order to avoid

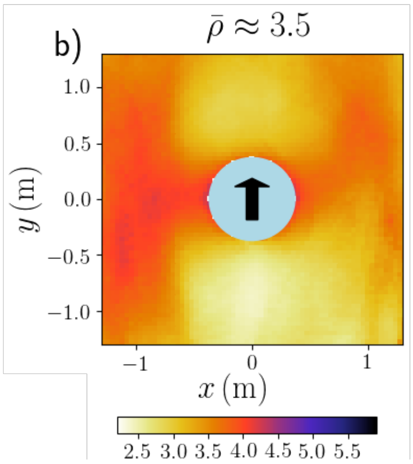

(a) Experimental density of pedestrians ($\bar{\rho} = m_0$).

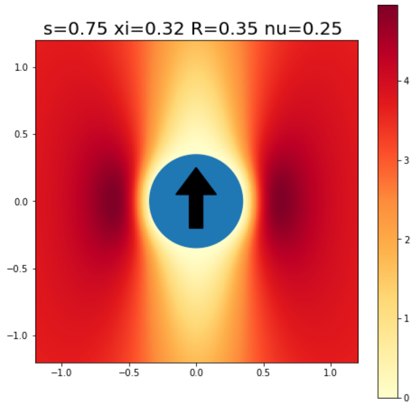

(b) Simulated density of pedestrians.

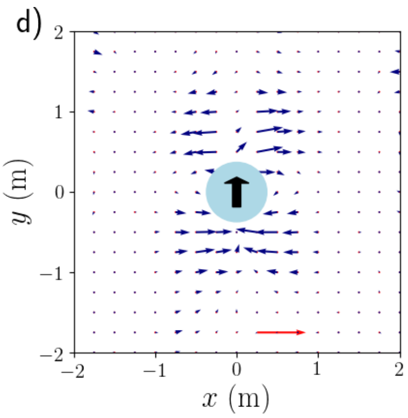

(c) Experimental velocity field.

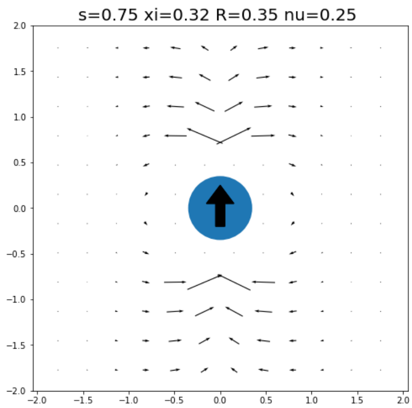

(d) Simulated velocity field.

Figure 7: Here are displayed both the density and the velocity field of the pedestrians. Our goal was to obtain a visually similar result to figure 3-b

this, therefore, a cutoff is introduced. Overall, what we have obtained is enough to conclude that our model simulates well the main experimental features.

I am personally rather satisfied with these results, especially since what we used is the simplest MFG model. This, however, is just the beginning of it. We are already working on substantial improvements. First of all, we asked ourselves how a *discount factor* can be introduced, in order to force agents to optimize their strategy not for the entire game but just considering what will happen in a finite future time span. Then, it is obvious that what we obtained here is a deterministic solution, coming from deterministic equations. However, the complexity of human behavior can hardly be described as deterministic. For this reason, our next goal will be to add some *randomness* to the equations. For example, we want to consider the case in which the velocity of the cylinder is not a constant but is a random variable. Finally, we would like to introduce *congestion effects*, that, as reported in [24], already helped describing interesting phenomena like the spontaneous appearance of preferential patterns of motion. The concept of congestion simply amounts to the fact that pedestrians collectively slow down in high density areas. We think that all these improvements of the model will help us reaching a deeper understanding of Mean-Field Games in general, and we hope will give us simulations closer to reality and with interesting emerging behaviors. We will see, however, what the future holds.

References

[1] Nicolas A., Kuperman M., Ibañez S., Bouzat S., and Appert-Rolland C. Mechanical response of dense pedestrian crowds to the crossing of intruders. *Scientific Reports*, 9(105), 2019.

[2] Seguin A., Bertho Y., Martinez F., Crassous Jèrôme, and Gondret P. Experimental velocity fields and forces for a cylinder penetrating into a granular medium. *Physical Review E*, 87(1):012201, 2013.

[3] Y. Achdou, F. J. Buera, J.-M. Lasry, Lions P.-L., and B. Moll. Partial differential equation models in macroeconomics. *Phil. Trans. R. Soc.*, 372, 2014.

[4] Y. Achdou, F. Camilli, and I. Capuzzo-Dolcetta. Mean field games: numerical methods for the planning problem.". *SIAM J. Control Optim.*, 50(1):77–109, 2012.

[5] Y. Achdou, P-N. Giraud, J.-M. Lasry, and P.-L. Lions. A long-term mathematical model for mining industries. *Appl. Math. Optim.*, 74:579–618, 2016.

[6] Yves Achdou, Martino Bardi, and Marco Cirant. Mean field games models of segregation. *Mathematical Models and Methods in Applied Sciences*, 27(01):75–113, 2017.

[7] Noha Almulla, Rita Ferreira, and Diogo Gomes. Two numerical approaches to stationary mean-field games. *Dynamic Games and Applications*, 7(4):657–682, 2017.

[8] R. Bellman, R.E. Bellman, and Rand Corporation. *Dynamic Programming*. Princeton University Press, 1957.

[9] A. Bensoussan, J. Frehse, and S. C. P. Yam. The master equation in mean field theory. *J. Math. Pures Appl.*, 103(6):1441–1474, 2015.

[10] Thibault Bonnemain, Thierry Gobron, and Denis Ullmo. Lax connection and conserved quantities of quadratic mean field games, 2020.

[11] P. Cardaliaguet. Notes on mean field games (from p.-l. lions' lectures at collège de france).

[12] P. Cardaliaguet and Lehalle C.-A. Mean field game of controls and an application to trade crowding, 2017.

[13] P. Cardaliaguet, J.-M. Lasry, P.-L. Lions, and A. Porretta. Long time average of mean field games with a nonlocal coupling. *SIAM J. Control Optim*, 51(5):3558–3591, 2013.

[14] Pierre Cardaliaguet, François Delarue, Jean-Michel Lasry, and Pierre-Louis Lions. *The Master Equation and the Convergence Problem in Mean Field Games*. Princeton University Press, 2019.

[15] R. Carmona and F. Delarue. Probabilistic analysis of mean-field games. *SIAM J. Control Optim.*, 51(4):2705–2734, 2013.

[16] René Carmona, François Delarue, and Aimé Lachapelle. Control of mckean–vlasov dynamics versus mean field games. *Mathematics and Financial Economics*, 7(2):131–166, 2013.

[17] Helbing D. *Physics of Dry Granular Media*. Springer, 1998.

[18] C.W. Gardiner. *Handbook of stochastic methods for physics, chemistry, and the natural sciences*. Springer-Verlag, 1985.

[19] D. A. Gomes and J. Saúde. Mean field games models – a brief survey. *J. Dyn. Games Appl.*, 4(2):110–154, 2014.

[20] O. Guéant. Mean field games equations with quadratic hamiltonian: a specific approach. *Math. Models Methods Appl. Sci.*, 22, 2012.

[21] M. Huang, R. P. Malhamé, and P. E. Caines. Large population stochastic dynamic games: closed-loop mckean–vlasov systems and the nash certainty equivalence principle. *Commun. Inf. Syst.*, 6(3):221–252, 2006.

[22] Arman C. Kizilkale and Roland P. Malhamé. Load shaping via grid wide coordination of heating-cooling electric loads: A mean field games based approach.

[23] Arman C Kizilkale, Rabih Salhab, and Roland P Malhamé. An integral control formulation of mean field game based large scale coordination of loads in smart grids. *Automatica*, 100:312–322, 2019.

[24] A. Lachapelle and M.-T. Wolfram. On a mean field game approach modeling congestion and aversion in pedestrian crowds. *Transportation Research Part B*, 45(10):1572–1589, 2011.

[25] J.-M. Lasry and P.-L. Lions. Jeux à champ moyen. i – le cas stationnaire. *C. R. Acad. Sci. Paris*, 343(9):619–625, 2006.

[26] J.-M. Lasry and P.-L. Lions. Jeux à champ moyen. ii – horizon fini et contrôle optimal. *C. R. Acad. Sci. Paris*, 343(10):679–684, 2006.

[27] J.-M. Lasry and P.-L. Lions. Mean field games. *Japanese Journal of Mathematics*, 2(1):229–260, 2007.

[28] Bain N. and Bartolo D. Dynamic response and hydrodynamics of polarized crowds. *Science*, 363(6422):46–49, 2019.

[29] C. J. Pethick and H. Smith. *Bose-Einstein Condensation in Dilute Gases*. Cambridge University Press, 2008.

[30] Faure S. and Maury B. Crowd motion from the granular standpoint. *Mathematical Models and Methods in Applied Sciences*, 25(03):463–493, 2015.

[31] Denis Ullmo, Igor Swiecicki, and Thierry Gobron. Quadratic mean field games. *Physics Reports*, 799:1–35, 2019.